



ELSEVIER

Polymer 43 (2002) 5133–5138

**polymer**[www.elsevier.com/locate/polymer](http://www.elsevier.com/locate/polymer)

# The effect of elastomeric nano-particles on the mechanical properties and crystallization behavior of polypropylene

Manli Zhang<sup>a</sup>, Yiqun Liu<sup>a</sup>, Xiaohong Zhang<sup>a</sup>, Jianming Gao<sup>a</sup>, Fan Huang<sup>a</sup>, Zhihai Song<sup>a</sup>,  
Genshuan Wei<sup>b</sup>, Jinliang Qiao<sup>a,\*</sup>

<sup>a</sup>SINOPEC Beijing Research Institute of Chemical Industry, Beijing 100013, People's Republic of China

<sup>b</sup>Institute of Applied Chemistry, College of Chemistry and Molecular Engineering, Peking University, Beijing 100080, People's Republic of China

Received 5 April 2002; received in revised form 25 May 2002; accepted 10 June 2002

## Abstract

Generally, toughness of polypropylene (PP) is an issue which has been investigated for many years to search for improvements. A traditional approach is to blend with rubber particles to enhance the toughness of PP yet modulus of PP decreases accordingly. Recently, we have achieved a good balance of toughness and stiffness of PP via blending PP with a small amount of elastomeric nano-particles (ENP). Based on our measurements, mechanical properties of the blends studied both the toughness of PP at room temperature and at  $-20\text{ }^{\circ}\text{C}$  show substantial increase. On the other hand, the stiffness of the PP blends retains or even possesses a slight enhancement. One of the reasons for this improvement is due to the fact that the ENP is not only a toughening modifier but also a nucleation agent for the PP. The nucleation density of the blends increases, while the crystallization kinetics of the blends becomes faster compared with the pure PP samples. © 2002 Elsevier Science Ltd. All rights reserved.

**Keywords:** Elastomeric nano-particles; Polypropylene; Crystallization, toughness and stiffness

## 1. Introduction

Isotactic polypropylene (PP) is a semi-crystalline polymer with desired properties, its toughness, especially notched impact strength, however, is not generally sufficient for applications as engineering plastics. Various methods for toughening PP have been studied, among which blending is the most effective and convenient way which can be classified into non-elastomer toughening [1,2] and elastomer toughening [3,4], or the combination of the both [5–7]. Recently, emerging is the method of rigid nano-particles toughening [8,9]. Toughen PP with some commonly used rubbers such as ethylene–propylene rubber (EPR), ethylene–propylene diene monomer (EPDM), and styrene–butadiene rubbers (SBR), can lead to fairly high toughness, but simultaneously the loss of stiffness cannot be neglected. While toughening PP with rigid particles, toughness cannot usually be improved effectively, although their tensile strength and stiffness increase. It is difficult to prepare a PP blend with good balance of toughness and stiffness.

Recently, a new kind of highly cross-linked nano-particle rubbers, ultra-fine full-vulcanized rubber powders (UFRP), by irradiating rubber latex and spray drying has been developed [10]. The particle size of the UFRP is tunable between 30 and 2000 nm by controlling polymerization conditions of the rubber latex. When the particle size is below 100 nm, the UFRP can be also recognized as elastomeric nano-particle (ENP). It has been found that the UFRP could be used in many different plastics as a good toughening modifier [11,12]. In this study, SB-ENP is used to toughen PP. A good combination of toughness and stiffness is achieved by blending PP with ENP.

According to the toughening theory [13,14], the formulation of

$$d_c = \tau_c / [k(\pi/6\Phi_r)^{1/3} - 1] \quad (1)$$

where  $d_c$  is the critical rubber particle diameter and  $\Phi_r$  the rubber volume fraction,  $k$  the geometric factor characterizing the spatial package of the particles,  $\tau_c$  is the critical face-to-face inter-particle distance or critical thickness of matrix ligaments. The brittle–tough transition occurs at a very low rubber volume fraction if the particle size of rubber is small enough. Therefore, the loss in stiffness caused by introducing

\* Corresponding author.

E-mail address: [jqiao@brici.ac.cn](mailto:jqiao@brici.ac.cn) (J. Qiao).

rubber into PP can be reduced effectively. However, the theory also indicates that adding rubber particles which are smaller than 100 nm does not toughen the PP materials.

In this paper we are going to show that a very low loading of the ENP can greatly improve the toughness of PP, and a reduction in stiffness of the composite caused by compounding a high rubber volume fraction can be avoided. We also found that ENP is a nucleation agent for PP crystallization.

## 2. Experimental section

### 2.1. Materials and specimen preparation

Materials used in this study included PP homopolymer (B-200) supplied by SINOPEC Luoyang PetroChem. China, and three kinds of styrene–butadiene ENP: DB-70 with 70 wt% butadiene, DB-50 with 50 wt% butadiene, and modified DB-50 ENP by spray drying DB-50 rubber latex together with dissolved sodium benzoate (10 phr based on dry latex).

Blends were prepared on a Werner and Pfeleiderer ZSK-25 co-rotating twin screw extruder with a barrel temperature of 190 °C and screw speed of 350 rpm. Specimens for impact strength tests (GB1843-93, 127 × 12.7 × 6.4 mm<sup>3</sup>), flexural strength tests (GB9341-2000, 120 × 10 × 4 mm<sup>3</sup>), heat distortion temperature (HDT) tests (GB1634-79, 120 × 10 × 4 mm<sup>3</sup>) and tensile strength tests (GB1040-92, 170 × 10 × 4) were injection-molded. The barrel and the nozzle temperatures of injection-molding machine were 220 and 240 °C, respectively. A single-edge 45° V-shaped notch (the tip radius = 0.25 mm and the depth = 2.5 mm) was milled in the specimens for impact tests.

### 2.2. Experimental measurements

#### 2.2.1. Particle, crystal, and texture observations

The appearance of ENP was observed with a JSM-35C scanning electron microscope (SEM) by dispersing the powder in ethanol, dropping it on the sample stage and then, coating the sample with gold. The binary phase structure of the composite was observed using an atomic force microscope (AFM) of Digital Instrumental in tapping mode. The sample was cryoultra-microtomed with a glass knife at about –100 °C to obtain a smooth surface for AFM observation. The crystalline structure was investigated with a SHIMADZU XRD-6000 diffractometer. The spherulite texture was observed with a Leitz SM-LUX polarization microscope (PLM); samples were melted at 230 °C for 2 min and then, isothermally crystallized in a vacuum oven.

#### 2.2.2. Mechanical properties

Tensile tests were carried out on an AG-1 tensile machine (50 mm/min). The impact strength was determined by Izod impact test on notched bars with a CEAST impact

machine. The flexural strength and modulus tests were carried out on Instron 4466. HDT was tested with a HD-PC Heat Distortion Tester.

### 2.2.3. Crystallization kinetics

Differential scanning calorimeter (DSC, Perkin–Elmer DSC 7) was used to determine crystallization parameters. General scan procedures were that samples were heated at 210 °C for 8 min in order to eliminate any thermal history of the material, and then, cooled to 50 °C at a rate of 10 °C/min, and held for 1 min at 50 °C. The samples were then heated from 50 to 210 °C at a heating rate of 10 °C/min. The peak temperatures of the corresponding exothermic and endothermic diagrams in these dynamic scans were taken as crystallization temperature,  $T_c$ , and melting temperature,  $T_m$ .

Isothermal crystallization experiments were performed as follows: the samples were heated at 210 °C for 8 min and then, quickly quenched (at a rate of 100 °C/min) to a preset isothermal crystallization temperature. The corresponding exothermal curves were recorded with respect to isothermal crystallization-time and normalized to the unit weight of the sample. All these procedures were carried out in a dry nitrogen atmosphere. The temperature calibration was conducted with the standard indium.

## 3. Results and discussion

### 3.1. Mechanical performances of the PP blends with elastomeric nano-particles

ENP is in a white powder form with good fluidity. Fig. 1 shows a SEM micrograph of DB-50 ENP. As shown in the figure, the particle size of ENP is very small with a few aggregates. Under a shear, the aggregates are easily to be separated in the PP melt during blending. This is due to a highly cross-linked structure within each nano-particles, which can effectively prevent the aggregates to be permanently sticking together in the blends.

Morphology of the binary structure in these blends is

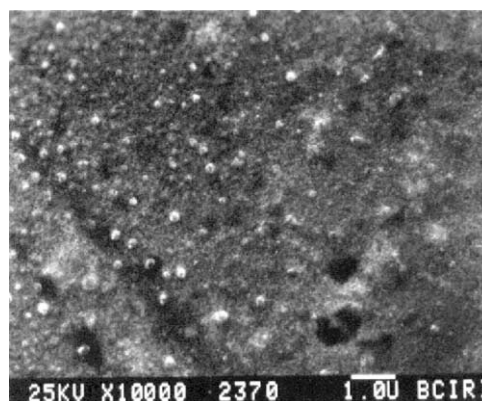


Fig. 1. SEM micrograph of DB-50 ENP.

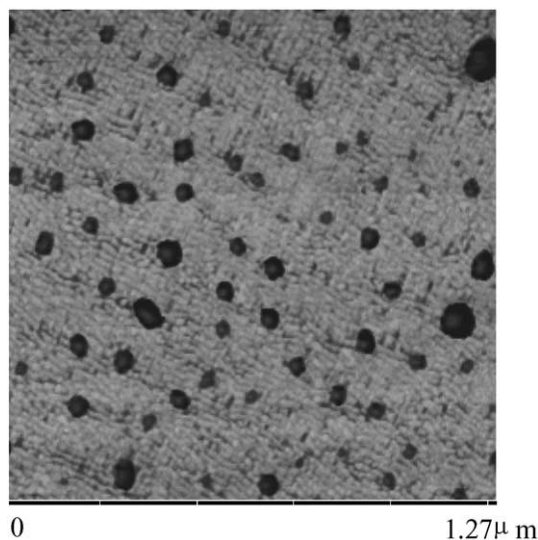


Fig. 2. AFM micrograph of PP toughened with 5 wt% modified DB-50 ENP.

observed in AFM. Fig. 2 is the micrograph of a PP blend toughened with a level of 5 wt% modified DB-50 ENP. It is evident that the nano-particles are well dispersed in PP matrix with a relatively monodisperse particle size below 100 nm. This may also be attributed to the better toughness of the PP blends in this case, since monodisperse particles could achieve more effectively in toughness than poly-disperse particles.

The mechanical properties of the PP toughened with modified DB-50 ENP are shown in Table 1. It is evident that even at a level of 2 wt% of ENP blended in the PP, the toughness and stiffness of the material can be effectively improved. The toughness of the blends drastically increases as the ENP content increases by a factor of 4.8 times. The tensile strength, flexural strength and modulus are on the other hand, retained or even slightly improved. The HDT also shows a 9 °C increase. Therefore, high toughness as well as a good balance in toughness and stiffness has been achieved. Note that these results cannot be obtained by blending commercially used rubber toughening agents.

It is known that PP possesses a low toughness, especially, at low temperatures. When PP is blended with DB-70 ENP which possesses a higher butadiene content, the mechanical properties of the blend are shown in Table 2. Specifically, the toughness of this blend both at -20 °C and room

temperature exhibits substantial improvements (1.7 times at room temperature and 1.2 times at -20 °C). The tensile strength, flexural strength and modulus in Table 2 are also evidently retained or slightly increased. Since the modulus of a blend is generally understood to be the linear addition with the fraction of the added component, adding rubber particles to PP should decrease the blend modulus. However, the PP blend toughened with DB-70 ENP shows a higher modulus compared with that of the pure PP. At the same time, the HDT of the blend also increases. In order to explain these experimental observations, a further investigation needs to be carried out on the crystallization behavior. We choose a typical blend of PP with 5 wt% DB-70 ENP as a representative and compare its crystallization behavior with the pure PP samples.

### 3.2. Dynamic crystallization behaviors

The crystallization temperature,  $T_c$ , the heat of crystallization,  $\Delta H_c$ , and the melting temperature,  $T_m$  are listed in Table 3. The corresponding DSC diagrams curves are shown in Fig. 3. It can be found that both  $T_c$  and  $T_m$  of the blends, especially the  $T_c$  value, clearly increases, and  $\Delta H_c$  of the blend, which has taken the fraction of the rubber nanoparticle weight into account, is also larger than that of pure PP. These data show that ENP may not only be a toughening agent, but also a nucleation agent in affecting the crystallization kinetics of PP. The  $T_m$  and  $\Delta H_c$  of blends, which were made by commercially available rubber toughening agents, are usually lower than those of pure PP, while the  $T_c$  does substantially increase [15–17]. It is thus obvious that the ENP must possess effects on toughness and nucleation, both of which significantly enhance the toughness and tensile properties. WAXD result shows that the crystals in both the blend and the pure PP belong to the identical monoclinic  $\alpha$  form as shown in Fig. 4 [18].

### 3.3. Isothermal crystallization kinetics and spherulitic morphology

The isothermal crystallization-time dependence at a constant  $T_c$  can be analyzed by the Avrami equation

$$1 - X(t) = \exp(-Kt^n) \quad (2)$$

where  $X(t)$  is the weight fraction of crystallized material at

Table 1  
Mechanical properties of PP toughened by modified DB-50 ENP

Sample	Tensile strength (MPa)	Notched Izod impact strength (J/m, 23 °C)	Flexural strength (MPa)	Flexural modulus (GPa)	HDT (°C)
Pure PP <sup>1</sup>	34.9	99.7	34.3	1.49	113.6
PP <sup>1</sup> /1 wt% ENP	36.6	105	37.2	1.62	124.8
PP <sup>1</sup> /2 wt% ENP	37.0	265	38.0	1.65	126.8
PP <sup>1</sup> /5 wt% ENP	35.7	479	35.9	1.58	122.5

<sup>1</sup>The ENP was modified by spray drying the DB-50 ENP latex together with dissolved sodium benzoate (10 phr based in dry latex). PP<sup>1</sup>: B-200 with MFI of 0.47 g/10 min at 230 °C.

Table 2  
Mechanical properties of PP toughened with 5 wt% DB-70 ENP

Sample	Tensile strength (MPa)	Notched Izod impact strength (J/m)	Flexural strength (MPa)	Flexural modulus (GPa)	HDT (°C)
Pure PP	34.9	99.7 (23 °C) 35.5 (−20 °C)	34.3	1.49	113.6
PP/5 wt% DB-70 ENP	35.4	167 (23 °C) 42.7 (−20 °C)	37.4	1.66	119.7

PP: B-200 with MFI of 0.7 g/10 min at 230 °C.

Table 3  
The results from DSC for pure PP and toughened PP

Sample	$T_c$ (°C)	$T_m$ (°C)	$-\Delta H_c$ (J/g)
Pure PP	111.1	162.7	89.4
PP/5 wt% DB-70 ENP	121.1	164.0	95.4

time  $t$ ,  $K$  is the overall crystallization rate constant and  $n$  the Avrami exponent. Here,  $X(t)$  is a value characterizing the relative crystallinity and defined as follows

$$X(t) = \frac{\int_0^t (d\Delta H/dt) dt}{\int_0^\infty (d\Delta H/dt) dt} \quad (3)$$

where the numerator is the heat generated due to crystallization at time  $t$ , and the denominator is the total heat when the crystallization is completed, both can be calculated from the recorded isothermal curves. The crystallization half-time ( $t_{1/2}$ ) at different  $T_c$ s, which is defined by the time at which 50% of the total crystallinity is reached, can be obtained. Fig. 5 shows two plots between reciprocal  $t_{1/2}$  and  $T_c$ . Note that  $1/t_{1/2}$  is proportional to the crystallization rate. It can be found that the crystallization rates of the blend in this whole  $T_c$  region studied are faster than those of the pure PP. When the logarithm of the Avrami equation is taken as follows:

$$\log\{-\ln[1-X(t)]\} = n \log t + \log K \quad (4)$$

The plots of  $\log\{-\ln[1-X(t)]\}$  versus  $\log t$  for the two

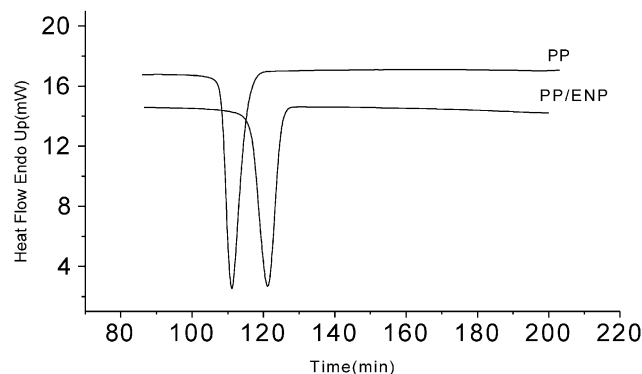


Fig. 3. Two DSC cooling crystallization diagrams at the rate of 10 °C/min for both the pure PP and PP toughened with 5 wt% DB-70 ENP.

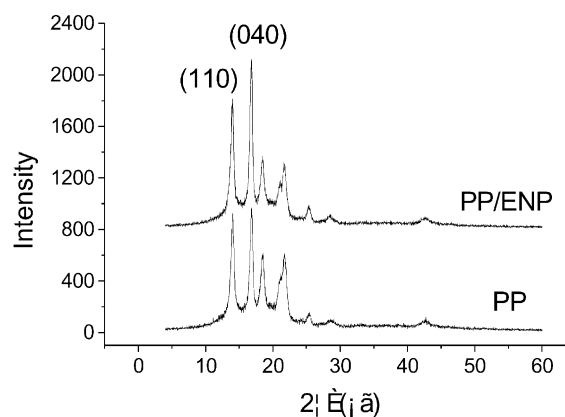


Fig. 4. Two WAXD patterns for both the pure PP and PP toughened with 5 wt% DB-70 ENP.

samples at different temperatures are shown in Fig. 6. It is evident that for the pure PP the plots exhibit straight lines in the whole crystallization-time region up to  $\log t = 0.5$ . For the blend (PP/5 wt% DB-70 ENP), a slope change takes place in the plots which occurs between  $\log t = -0.5$  and 0 in the late stage of the crystallization process. It has been identified that in PP this slope change is associated with the impingement of neighboring spherulites, and thus, represents a beginning of secondary crystallization [19]. This indicates that the density of spherulites in the blend, which reflects the nucleation density of the PP, increases as

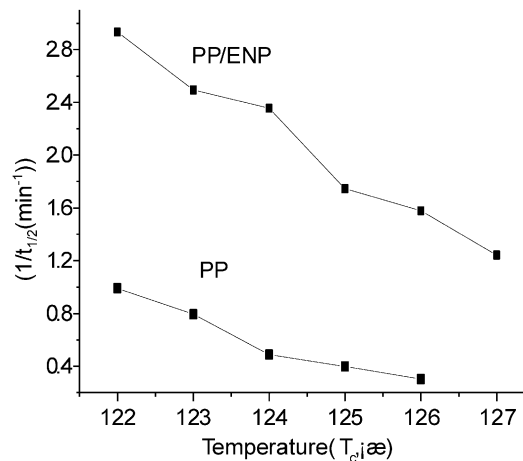


Fig. 5. The reciprocal of half-time of crystallization ( $t_{1/2}$ ) versus crystallization temperatures for both the pure PP and PP toughened with 5 wt% DB-70 ENP.

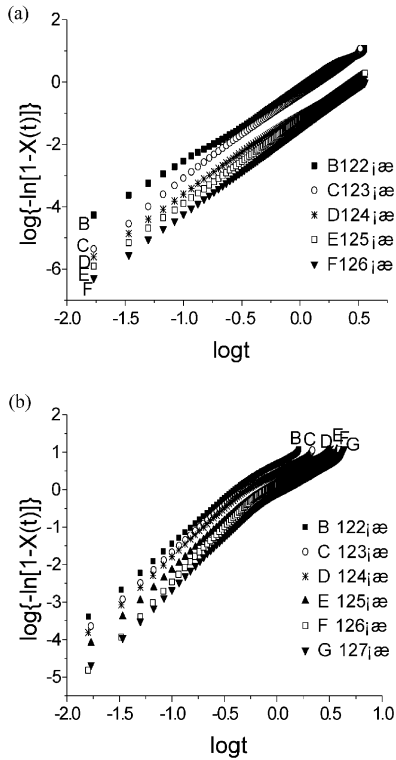


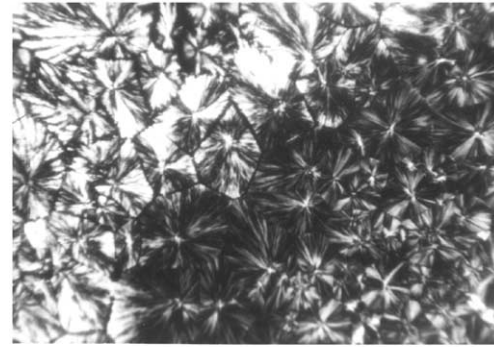
Fig. 6. The plots of  $\log\{-\ln[1-X(t)]\}$  versus  $\log t$  at various temperatures: (a) PP and (b) PP/ENP.

directly visualized in PLM (Fig. 7). The observation indicates that the spherulitic size in the blend is much smaller than that of the pure PP, as shown in Fig. 7.

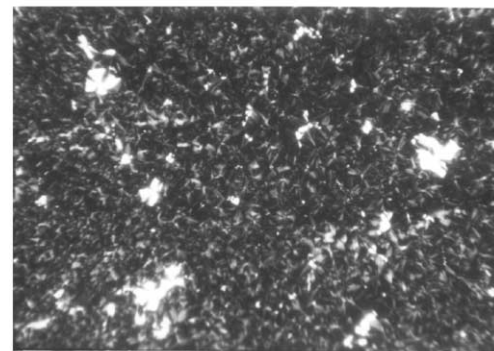
Table 4 illustrates the slope and intercept of the plots in Fig. 6, which are used to calculate the values of  $K$  and  $n$  (also included in Table 4). The rate constant  $K$  and the Avrami exponent  $n$  can be used to interpret qualitatively the nucleation mechanism and overall crystallization rate of polymer, respectively. It can be found in Table 4 that the Avrami exponents are between 2 and 3, inferring that spherulitic development arises from an athermal heterogeneous nucleation [20]. It can also be found that the rate constants of the blend at all  $T_c$ s studied are higher than those of the pure PP at the corresponding  $T_c$ s. With increasing

Table 4  
Kinetics parameters analyzed by the Avrami equation

Sample	$T_c$ (°C)	$n$	$K$ (min <sup>-n</sup> )	$t_{1/2}$ (min)
Pure PP	122	2.43	0.675	1.01
	123	2.63	0.374	1.26
	124	2.60	0.107	2.05
	125	2.63	0.062	2.51
	126	2.61	0.031	3.31
PP/5 wt% DB-70 ENP	122	2.44	9.55	0.341
	123	2.54	7.06	0.401
	124	2.59	6.40	0.425
	125	2.61	2.97	0.573
	126	2.87	2.57	0.634
	127	2.74	1.25	0.806



(a)



(b)

Fig. 7. PLM micrographs for (a) the pure PP and (b) PP toughened with 5 wt% DB-70 ENP crystallized at 118 °C for 5 h.

isothermal  $T_c$ , the Avrami exponent slightly increases while the rate constant decreases and consequently  $t_{1/2}$  increases.

The temperature dependence of crystallization rate constant of both samples is compared by means of the activation energy, which can be obtained from the slopes of the plots of  $\ln K$  versus  $(1/T)$  (Table 4) according to the Arrhenius equation

$$K = A_0 \exp(-E_a/RT) \quad (5)$$

Fig. 8 shows that the activation energy of the blend is smaller than that of the pure PP, revealing a less temperature dependence of crystallization rate constant of the blend. Furthermore, the difference between these two rate constants for the blend and the pure PP becomes widened with increasing  $T_c$ . It can thus be reasonably deduced that

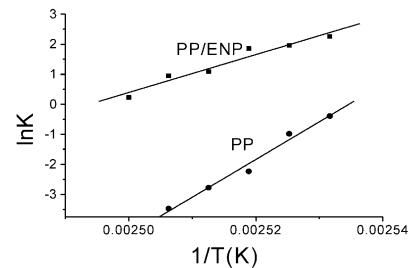


Fig. 8. Activation energies of the overall crystallization change with crystallization temperatures for the pure PP and the PP toughened with 5 wt% DB-70 ENP.

ENP may act as nucleation agents to form heterogeneous nuclei which is more effective at higher  $T_c$ s.

It is believed that in general, a higher spherulite density also helps to improve materials' toughness. On the other hand, modulus of materials is usually more critically associated with crystallinity in a small (linear) deformation region where the modulus is measured, and less affected by the crystalline morphology. However, in this study, it has been shown that crystal morphology may also substantially influence the materials' modulus.

#### 4. Conclusion

In summary, we have reported a novel class of elastomeric rubber nano-particles, ENP, which can effectively toughen PP due to its small particle size, and uniform dispersion. Blending PP with a low volume fraction of ENP can lead to substantial enhancements of the toughness and their stiffness. Furthermore, these nano-particles can also serve as nucleation agents to speed up the crystallization kinetics of PP. The crystallization rate, crystallinity, and nucleation density of PP in the blend increases, and they may serve as one of the reasons to achieve a balanced toughness and stiffness of the PP.

#### Acknowledgments

Subsidized by the Special Funds for Major State Basic Research Projects G1999064800.

#### References

- [1] Kurauchi T, Ohta T. *J Mater Sci* 1984;19:1699.
- [2] Li DM, Qi ZN. *Symp 37th Polym Semin Jpn* 1988;37:2339.
- [3] Karger-Kocsis J, Kallo A, Szafner A, Bodor G, Sényei Zs. *Polymer* 1979;20:37.
- [4] Bucknall CB. *Toughened plastics*. London: Applied Science; 1977.
- [5] Ou Y, Fang X, Feng Y. *Acta Polym Sin Chin* 1996;5:601.
- [6] Zhang Y, Chen R, Zheng H. *Polym Mater Sci Engng Chin* 1998;5:128.
- [7] Kolařík J, Jančá J. *Polymer* 1992;33:4961.
- [8] Kurokawa Y, Yasuda H, Kashiwagi M, Oyo A. *J Mater Sci Lett* 1997;16:1670.
- [9] Hasegawa N, Kawasumi M, Kato M, Usuki A, Okada A. *J Appl Polym Sci* 1998;67:87.
- [10] Qiao J, Wei G, Zhang X, Liu Y. *PCT/CN00/00281*.
- [11] Liu Y, Zhang X, Wei G, Gao J, Huang F, Zhang M, Guo M, Qiao J. *Chin J Polym Sci* 2002;20:93.
- [12] Qiao J, Zhang X, Liu Y, Wei G, Zhang Sh, Zhang M, Gao J, Huang F. *Symp Polym Sci Chin* 2001;G-243.
- [13] Wu S. *J Appl Polym Sci* 1988;35:549.
- [14] Wu S. *Polymer* 1985;26:1855.
- [15] Jang BZ. *J Appl Polym Sci* 1984;29:4377.
- [16] Jang BZ. *J Appl Polym Sci* 1985;30:2485.
- [17] Xu M, Hu Sh, Zhang X, Guan J. *Polym Commun Chin* 1981;5:339.
- [18] Janimak JJ, Cheng SZD, Zhang A, Hsieh ET. *Polymer* 1992;33:728.
- [19] Wunderlich B. *Macromolecular physics. Crystal nucleation, growth and annealing*, vol. II. New York: Academic Press; 1976. chapter 6.
- [20] Avalos F, Lopez-Manchado M, Arroyo M. *Polymer* 1998;39:6173.